



## Negative refraction by a planar Ag/SiO<sub>2</sub> multilayer at ultraviolet wavelength to the limit of silver

J. Zhao, J. Gao, Y. Deng, H. Liu, and X. Wang

Citation: *AIP Advances* **4**, 047127 (2014); doi: 10.1063/1.4873156

View online: <http://dx.doi.org/10.1063/1.4873156>

View Table of Contents: <http://scitation.aip.org/content/aip/journal/adva/4/4?ver=pdfcov>

Published by the [AIP Publishing](#)

---

### Articles you may be interested in

Fabrication of large-area 3D optical fishnet metamaterial by laser interference lithography

*Appl. Phys. Lett.* **103**, 123116 (2013); 10.1063/1.4821508

High quality transparent TiO<sub>2</sub>/Ag/TiO<sub>2</sub> composite electrode films deposited on flexible substrate at room temperature by sputtering

*APL Mat.* **1**, 012102 (2013); 10.1063/1.4808438

Enhanced high thermal conductivity and low permittivity of polyimide based composites by core-shell Ag@SiO<sub>2</sub> nanoparticle fillers

*Appl. Phys. Lett.* **101**, 012903 (2012); 10.1063/1.4733324

In situ optical microspectroscopy approach for the study of metal transport in dielectrics via temperature- and time-dependent plasmonics: Ag nanoparticles in SiO<sub>2</sub> films

*J. Chem. Phys.* **134**, 054707 (2011); 10.1063/1.3537736

Multilayer high reflectance coating on polyethylene terephthalate film consisting of Ag / SiO<sub>2</sub> / TiO<sub>2</sub> layers that are not quarter-wave thickness

*J. Vac. Sci. Technol. A* **28**, 99 (2010); 10.1116/1.3269736

---



## Negative refraction by a planar Ag/SiO<sub>2</sub> multilayer at ultraviolet wavelength to the limit of silver

J. Zhao,<sup>1,2</sup> J. Gao,<sup>1,a</sup> Y. Deng,<sup>2,3</sup> H. Liu,<sup>1</sup> and X. Wang<sup>1</sup>

<sup>1</sup>Key Laboratory for Optical System Advanced Manufacturing Technology, Changchun Institute of Optics, Fine Mechanics and Physics, Chinese Academy of Sciences, 3888 Dongnanhu Road, Changchun, Jilin, 130033, P. R. China

<sup>2</sup>University of Chinese Academy of Sciences, Beijing, 100039, China

<sup>3</sup>State Key Laboratory of Luminescence and Applications, Changchun Institute of Optics, Fine Mechanics and Physics, Chinese Academy of Sciences, 3888 Dongnanhu Road, Changchun, Jilin, 130033, P. R. China

(Received 22 October 2013; accepted 14 April 2014; published online 22 April 2014)

For planar structured hyperbolic metamaterial, the shortest wavelength achievable for negative refraction is often limited by dielectric layers, which are usually wide band gap semiconductors that absorb light strongly at wavelength shorter than their absorption edge. Here we proposed that using SiO<sub>2</sub> may break such limitation based on effective medium theory. Through calculation and simulation we demonstrated broad angle negative refraction by a planar Ag/SiO<sub>2</sub> layered structure at wavelength down to 326 nm. Its imaging and focusing abilities were also presented. The lower limit of wavelength here is defined by the property of silver, whose permittivity turns positive below 324 nm. © 2014 Author(s). All article content, except where otherwise noted, is licensed under a Creative Commons Attribution 3.0 Unported License. [<http://dx.doi.org/10.1063/1.4873156>]

Manipulating light in the ultraviolet regime with subwavelength resolution can promote the development of photolithography, ultraviolet optoelectronic devices and fluorescence imaging. The “left-handed” material, which processes negative permittivity ( $\epsilon < 0$ ) and negative permeability ( $\mu < 0$ ) simultaneously, would generate negative refractive index that is critical for subwavelength resolution.<sup>1,2</sup> People have demonstrated artificial two or three dimensional periodic structures for negative refraction from microwave to near-infrared regime.<sup>3,4</sup> However, scaling down these structures into sub-micrometer scale for visible and ultraviolet light is restricted by current nanofabrication techniques.<sup>5</sup> To release such constriction, Pendry pointed out that, since electric and magnetic fields decouple in the near field, for transverse magnetic (TM) polarized wave, only  $\epsilon < 0$  is required for negative refractive index.<sup>6</sup> Metals have  $\epsilon < 0$  in the visible and ultraviolet regime, thus a periodic one dimensional metal-dielectric layered structure has been proposed to realize negative refraction, with efficient transmission through evanescent wave coupling between nearby layers.<sup>7</sup> There are two configurations of such “hyperbolic metamaterial”,<sup>8</sup> as shown in Figs. 1(a) and 1(b). The planar structure (Fig. 1(a)) has highly practical significance, since it is readily achievable by current thin film deposition techniques.

This planar structure, however, places additional requirements on material selection. The dispersion relation for hyperbolic metamaterial is given by:

$$\frac{k_x^2}{\epsilon_z} + \frac{k_z^2}{\epsilon_x} = k_0^2 \quad (1)$$

where  $k_0$  is the wave vector in free space;  $k_x$  and  $k_z$  are wave vectors in the metamaterial along x and z directions respectively;  $\epsilon_x$  and  $\epsilon_z$  are the effective permittivities of the metamaterial along x and z directions respectively. Negative refraction could occur only if  $\epsilon_z \epsilon_x < 0$ ,<sup>9</sup> which corresponds

<sup>a</sup>Author to whom correspondence should be addressed. Electronic mail: [gaojs@ciomp.ac.cn](mailto:gaojs@ciomp.ac.cn)



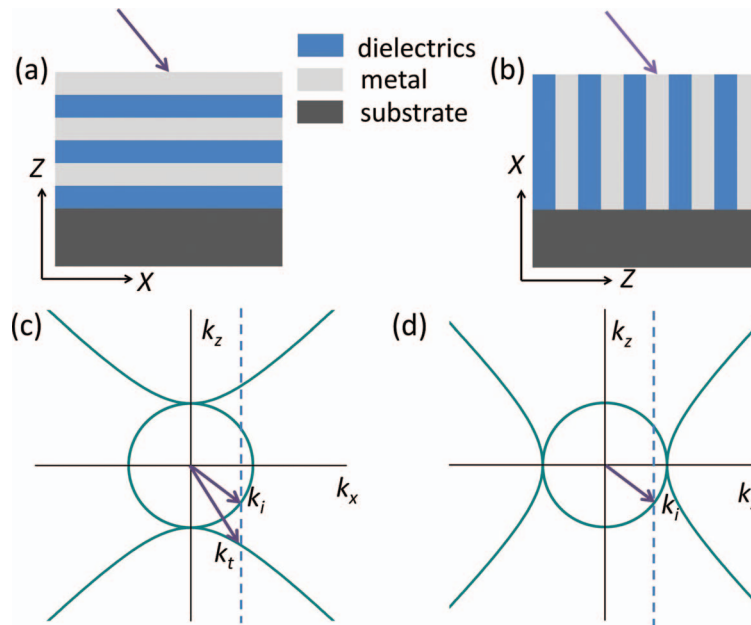


FIG. 1. (a) Planar and (b) vertical structured hyperbolic metamaterial. (c) Hyperbolic dispersion relation with  $\epsilon_x > 0$ ,  $\epsilon_z < 0$ . (d) Hyperbolic dispersion relation with  $\epsilon_x < 0$ ,  $\epsilon_z > 0$ . The circles in (c) and (d) represent the dispersion relation of free space.

to a hyperbola that “sits” on either  $k_z$  or  $k_x$  axis, as shown in Figs. 1(c) and 1(d) respectively. But to realize the planar structure, which means the light can be bent negatively when incident on the metamaterial’s surface parallel to  $k_x$ , the hyperbola needs to “sit” on  $k_z$  axis (Fig. 1(c)) to satisfy the conservation of  $k_x$ . Otherwise, as the case of Fig. 1(d), incident light will be bifurcated into two refractive waves propagating into opposite directions along the  $k_x$  axis to conserve  $k_x$ .<sup>10,11</sup> When  $\epsilon_x > 0$  and  $\epsilon_z < 0$ , the hyperbola “sits” on  $k_z$  axis. According to the effective medium theory,<sup>9</sup> when the layer is much thinner than the incident wavelength ( $< 1/10 \lambda$ ),  $\epsilon_x$  and  $\epsilon_z$  can be expressed as follows:

$$\epsilon_x = f\epsilon_m + (1 - f)\epsilon_d \quad (2)$$

$$\epsilon_z = \frac{1}{f\epsilon_m^{-1} + (1 - f)\epsilon_d^{-1}} \quad (3)$$

where  $f$  is the filling ratio of metal, defined by the ratio between the total thickness of metal to the total thickness of the metamaterial;  $\epsilon_m$  and  $\epsilon_d$  are the real part of permittivity of metal and dielectric, respectively. Considering that  $0 < f < 1$ , to achieve  $\epsilon_x > 0$  and  $\epsilon_z < 0$ , the choice of metal and dielectric must meet  $\epsilon_d\epsilon_m < 0$  and  $-\epsilon_m < \epsilon_d$ .

Normally the minus real part of permittivity of noble metals  $-\epsilon_m$  (e.g. Ag, which has relatively low loss from visible to ultraviolet wavelength range) is much larger than the permittivity of commonly available dielectric materials  $\epsilon_d$  in visible frequency, leading to the dispersion relation in Fig. 1(d). This may explain why negative refraction in visible range usually relies on the vertical structure as in Fig. 1(b).<sup>12,13</sup> For Ag, the value of  $-\epsilon_m$  decreases from visible to ultraviolet wavelength, providing the opportunity for dielectric materials with high permittivity ( $\epsilon_d > 5$ ) to satisfy  $-\epsilon_m < \epsilon_d$ . That’s why planar structures are usually realized in ultraviolet regime.<sup>14–17</sup> However, in real situation, many of those dielectric materials with high permittivity such as Zinc Oxide or Titanium Dioxide are wide band gap semiconductors that they have strong absorption at wavelengths shorter than their absorption edge (commonly longer than 340 nm), which defines the lower limit of wavelength of effective negative refraction.<sup>14</sup> Therefore, to realize negative refraction at even shorter wavelength is still a challenge.

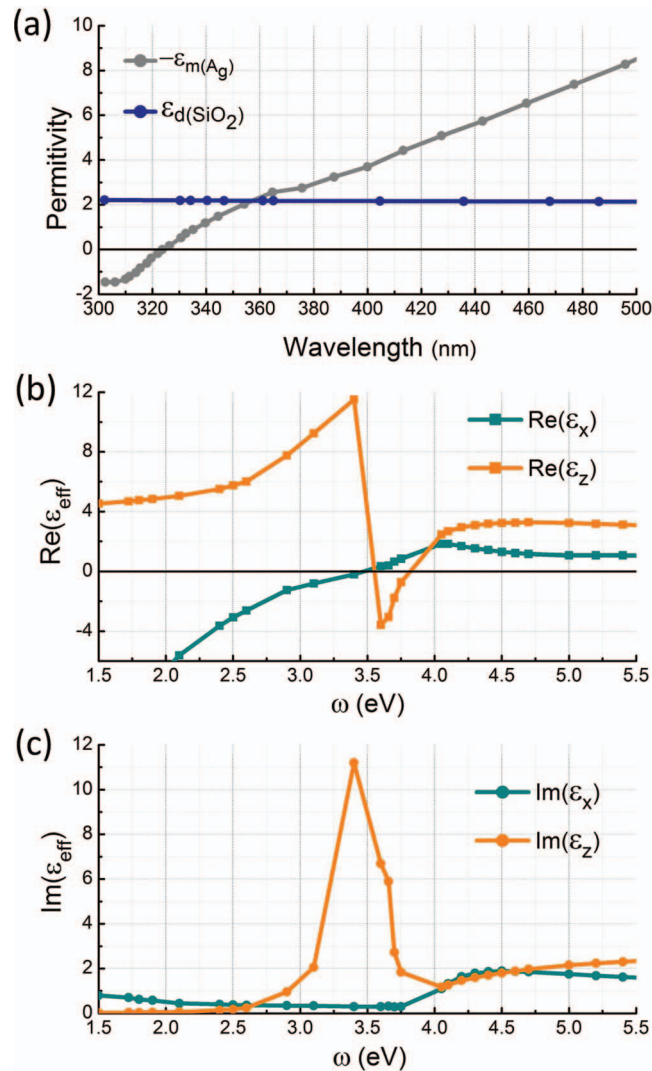


FIG. 2. (a) The real part of permittivity of  $\text{SiO}_2$  ( $\epsilon_{\text{SiO}_2}$ ) and Ag ( $-\epsilon_{\text{Ag}}$ ) as a function of different wavelengths. (b) The real part and (c) the imaginary part of permittivity of  $\epsilon_x$  and  $\epsilon_z$  of a planar Ag/ $\text{SiO}_2$  layered structure with  $f = 0.5$  versus photon energy (eV).

Here we try to explore the possibility of using  $\text{SiO}_2$  as the dielectric layer, which though has much smaller permittivity, is transparent to ultraviolet light at wavelengths down to 160 nm. The dependence of the real part of permittivity of  $\text{SiO}_2$  ( $\epsilon_{\text{SiO}_2}$ ) and Ag ( $-\epsilon_{\text{Ag}}$ ) on the wavelength are shown in Fig. 2(a), calculated from their respective refractive index data edited by Palik.<sup>18</sup> With the wavelength decreases from 500 nm to 300 nm,  $\epsilon_{\text{SiO}_2}$  is around 2.1, but  $\epsilon_{\text{Ag}}$  progressively decreases and becomes smaller than  $\epsilon_{\text{SiO}_2}$  at the wavelength around 360 nm. Therefore, negative refraction is possible for Ag/ $\text{SiO}_2$  system at wavelengths below 360 nm. It should be noted that  $\epsilon_{\text{Ag}}$  becomes positive at wavelengths below 324 nm, which sets the lower limit of negative refraction with Ag as the metal layer.

Now we consider a planar Ag/ $\text{SiO}_2$  layered structure with  $f = 0.5$ . The real parts of  $\epsilon_x$  and  $\epsilon_z$  calculated from Eqs. (2) and (3) are shown in Fig. 2(b). Because of limited data, the plot is dispersive. But we can still find that the situation of  $\text{Re}(\epsilon_x) > 0$  and  $\text{Re}(\epsilon_z) < 0$  exists roughly between 3.55 eV and 3.80 eV, indicating that negative refraction may be obtained at wavelengths ranging from 326 to 350 nm. The imaginary parts of  $\epsilon_x$  and  $\epsilon_z$  calculated from Eqs. (2) and (3) are shown in Fig. 2(c).  $\text{Im}(\epsilon_x)$  increases with the photon energy from 3.75 eV, suggesting increased transverse absorption at wavelengths shorter than 330 nm. On the other hand,  $\text{Im}(\epsilon_z)$  increases rapidly as the photon energy

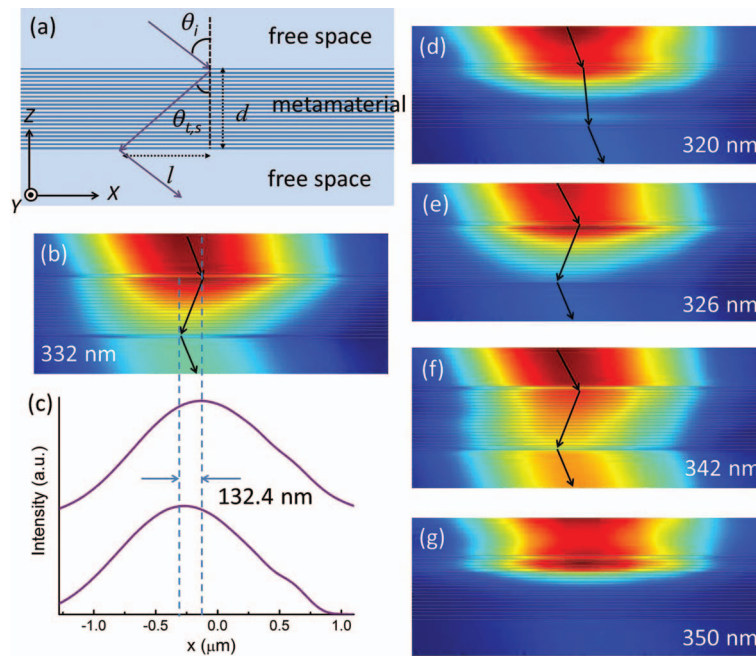


FIG. 3. (a) Simulation configuration where the structure is composed of planar Ag/SiO<sub>2</sub> periodic layers with each layer of 5 nm thick and totally 20.5 periods. A Gaussian TM polarized light propagating through the structure with a negative refraction is illustrated. (b) Simulated result of electric field intensity distribution for incident light with wavelength of 332 nm. (c) The 332 nm beam's intensity profiles on the upper and lower surfaces of the metamaterial. (d-g) Simulated results of electric field intensity distribution for incident light with wavelengths of 320 nm, 326 nm, 342 nm and 350 nm.

decreases from 3.7 eV, thus the longitudinal transmission loss is getting much higher at even longer wavelengths.

The negative refraction ability of the structure is investigated by finite-difference time-domain method. The slab for simulation contains alternate layers of Ag and SiO<sub>2</sub> with each layer of 5 nm thick and totally 20.5 periods (Fig. 3(a)). The number of periods chosen is to demonstrate obvious negative refraction effect (with sufficient light beam shift but less loss), and other number of periods works as well. The light source is a Gaussian TM polarized wave with an incident angle of 40°. The results are shown in Figs. 3(b)–3(g). At the wavelength of 320 nm, the refraction is positive (Fig. 3(d)), because the permittivity of Ag is positive here. At 350 nm, the light cannot propagate through the metamaterial (Fig. 3(g)), as the longitudinal loss is high. From 326 nm to 342 nm, negative refraction is observed (Figs. 3(b), 3(e), and 3(f)), agrees well with our estimation. The transmission at 326 nm is much lower than that at 332 nm and 342 nm, which is contributed to the high transverse loss at 326 nm as we have pointed out. In following sections, we choose 332 nm as the wavelength of the light source.

Figure 3(c) shows the beam's intensity profiles on the two interfaces of the metamaterial in Fig. 3(b). It is observed that the incident light can be shifted by  $-132.4$  nm. In addition, the metamaterial has a total thickness of 205 nm and the incident angle is 40°. Therefore, according to Snell's law, we can obtain the effective refractive index  $n_{eff}$  of the metamaterial, which is  $-1.19$ . Based on the same calculation, we further changed the incident angle from 20° to 50° by an interval of 5° and we obtained different  $n_{eff}$ , as are plotted in Fig. 4 by the squares.

The relationship between  $n_{eff}$  and  $\theta_i$  can also be theoretically derived from the dispersion relation and Snell's law:

$$n_{eff} = \frac{\sin(\theta_i)}{\sin\left(-\tan^{-1}\left(\sin(\theta_i)\sqrt{\frac{\epsilon_x}{\epsilon_z(\epsilon_z - \sin^2(\theta_i))}}\right)\right)} \quad (4)$$

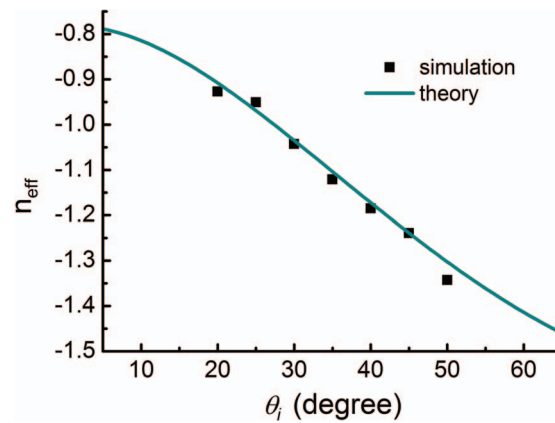


FIG. 4. The relationship between incident angle  $\theta_i$  and effective refractive index  $n_{\text{eff}}$  obtained from theory (solid line) and simulation results (squares).

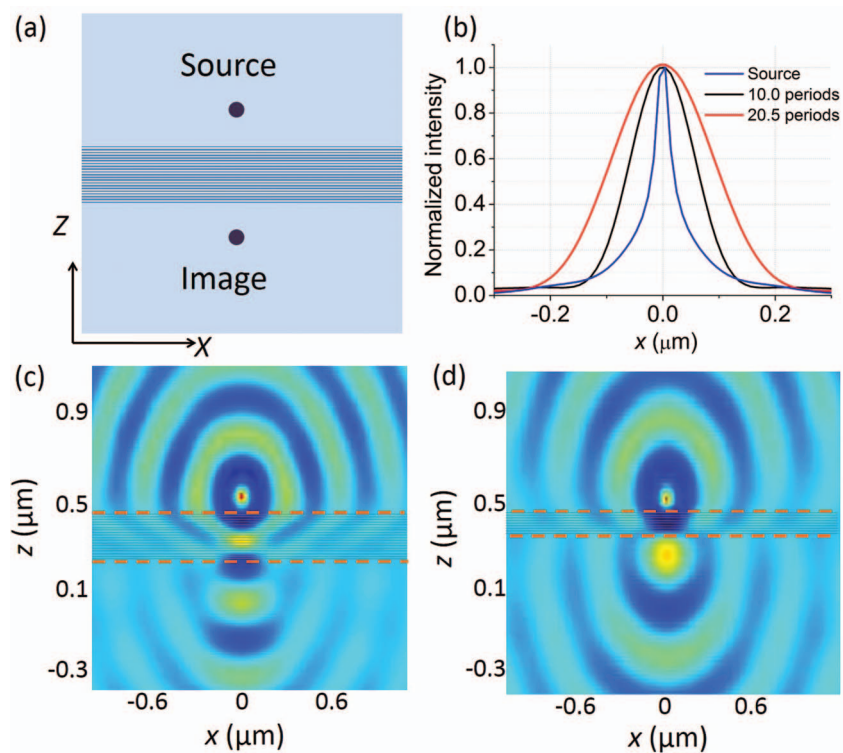


FIG. 5. (a) Illustration for the imaging of the metamaterial slab. (b)  $|H_y|^2$  distribution in the source plane and in the image plane of metamaterial slabs with 10 and 20.5 periods. (c) The simulated result of phase wave front of  $H_y$  distribution with a point source placed 100 nm above a metamaterial slab with 20.5 periods. (d) The simulated result of phase wave front of  $H_y$  distribution with a point source placed 50 nm above a metamaterial slab with 10 periods.

which is also drawn in Fig. 4 by the solid line. We can see that the theoretical plot fits well with the simulation results. The metamaterial realizes effective negative refraction over a broad incident angle from  $20^\circ$  to  $50^\circ$ , with  $n_{\text{eff}}$  increases from  $-0.93$  to  $-1.34$ .

A metamaterial with  $n_{\text{eff}}$  around  $-1$  is desirable for imaging and focusing.<sup>6,14,19</sup> In Fig. 5(a), a point source is placed 100 nm above the metamaterial slab. From the distribution of phase wave front of  $H_y$  as shown in Fig. 5(c), we can see that an image is formed on the other side of the slab. The distance between source and image is measured to be 486 nm, which is close to  $2d$  (410 nm). This

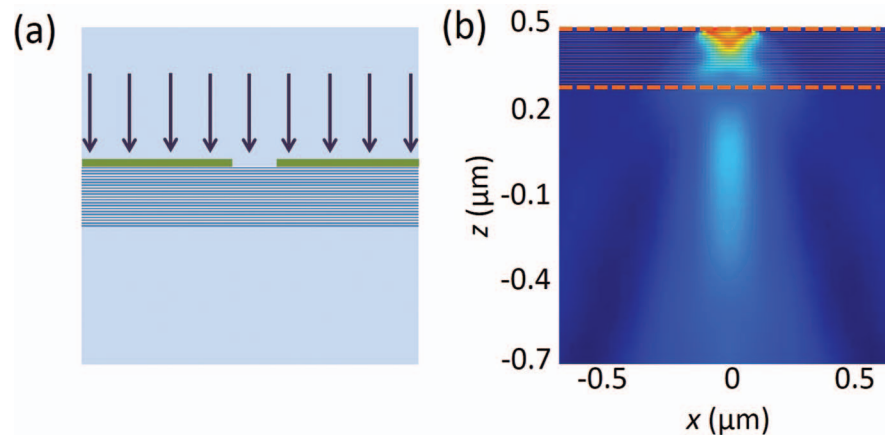


FIG. 6. (a) A TM polarized plane wave incident onto the slab with 20.5 periods through a 165 nm wide aperture on Cr mask. (b) The simulated result of power distribution.

further support that the refractive index of our metamaterial is near  $-1$ .<sup>20</sup> If we move the position of source, the image will move accordingly, keeping their distance to be near  $2d$ , but the imaging quality would not change.

It should be noted that the feature size of the image is larger than the source spot. This is because when using real material (Ag and SiO<sub>2</sub> in our case) to construct negative refraction metamaterial, the evanescent wave that contributes to super-resolution is eliminated because of the high loss of real material.<sup>21</sup> Similar results are obtained elsewhere using real material as well.<sup>13,22,23</sup> If we reduce the thickness of metamaterial to 10 periods, the absorption loss is reduced and the imaging ability is improved (Fig. 5(d)). As is shown in Fig. 5(b), the full width half maximum (FWHM) is reduced from  $0.61\lambda$  of 20.5 periods to  $0.39\lambda$  of 10 periods, realizing superdiffraction limit imaging.<sup>13</sup>

Furthermore, when applying a TM polarized plane wave onto the slab through a 165 nm wide aperture on a Chromium mask (Fig. 6(a)), a focus below the slab is observed from the power distribution (Fig. 6(b)), showing the flat focusing ability of the metamaterial. The elongation of the focus point results from the angle-dependent  $n_{eff}$  (Fig. 4).<sup>12</sup>

In summary, we have realized effective ultraviolet negative refraction by a planar Ag/SiO<sub>2</sub> layered structure at wavelength down to the limit of Ag, whose permittivity turns positive below 324 nm. Because of the transparency of SiO<sub>2</sub> in ultraviolet regime, the previous wavelength limitation that using wide band gap semiconductors as the dielectric layers has strong absorption effect is circumvented. Theoretical calculation and numerical simulation show broad angle negative refraction by the structure for TM-polarized light from 342 nm to 326 nm with an effective refractive index around  $-1$ . The imaging and focusing abilities have also been demonstrated. To realize negative refraction at even shorter wavelength, alternative metals need to be considered. This work may lead to a clear direction for choosing real materials to constitute the desirable hyperbolic metamaterial.

The authors acknowledge the support from the Innovation Foundation of the Key Laboratory of the Chinese Academy of Sciences under grant numbers of Y2GX1SJ134.

<sup>1</sup> V. G. Veselago, *Sov. Phys. Usp.* **10**, 509 (1968).

<sup>2</sup> X. Zhang and Z. Liu, *Nat. Mater.* **7**, 435 (2008).

<sup>3</sup> R. A. Shelby, D. R. Smith, and S. Schultz, *Science* **292**, 77 (2001).

<sup>4</sup> S. Zhang, W. Fan, N. C. Panoiu, K. J. Malloy, R. M. Osgood, and S. R. J. Brueck, *Phys. Rev. Lett.* **95**, 137404 (2005).

<sup>5</sup> V. M. Shalaev, *Nature Photon.* **1**, 41 (2007).

<sup>6</sup> J. B. Pendry, *Phys. Rev. Lett.* **85**, 3966 (2000).

<sup>7</sup> S. A. Ramakrishna, J. B. Pendry, M. C. Wiltshire, and W. J. Stewart, *J. Mod. Opt.* **50**, 1419 (2003).

<sup>8</sup> M. Noginov, M. Lapine, V. Podolskiy, and Y. Kivshar, *Opt. Express.* **21**, 14895 (2013).

<sup>9</sup> B. Wood, J. B. Pendry, and D. P. Tsai, *Phys. Rev. B.* **74**, 115116 (2006).

<sup>10</sup> B. Zeng, X. Yang, C. Wang, Q. Feng, and X. Luo, *J. Opt.* **12**, 035104 (2010).

<sup>11</sup> Y. Zhao, A. A. Nawaz, S. S. Lin, Q. Hao, B. Kiraly and T. J. Huang, *J. Phys. D: Appl. Phys.* **44**, 415101 (2011).

<sup>12</sup> Y. Liu, G. Bartal, and X. Zhang, *Opt. Express.* **16**, 15439 (2008).

- <sup>13</sup>X. B. Fan, G. P. Wang, J. C. W. Lee, and C. T. Chan, *Phys. Rev. Lett.* **97**, 073901 (2006).
- <sup>14</sup>T. Xu, A. Agrawal, M. Abashin, K. J. Chau and H. J. Lezec, *Nature*. **497**, 470 (2013).
- <sup>15</sup>N. Fang, H. Lee, and X. Zhang, *Science*. **308**, 534 (2005).
- <sup>16</sup>D. O. S. Melville, R. J. Blaikie, and C. R. Wolf, *Opt. Express*. **13**, 2127 (2005).
- <sup>17</sup>E. Verhagen, R. Waele, L. Kuipers, and A. Polman, *Phys. Rev. Lett.* **105**, 223901 (2010).
- <sup>18</sup>*Handbook of Optical Constants of Solids*, edited by E. D. Palik (Academic Press, London, 1985).
- <sup>19</sup>W. T. Lu and S. Sridhar, *Phys. Rev. B*. **77**, 233101 (2008).
- <sup>20</sup>D. R. Smith, J. B. Pendry, and M. C. K. Wiltshire, *Science*, **305**, 788 (2004).
- <sup>21</sup>D. R. Smith, D. Schurig, M. Rosenbluth, S. Schultz, S. Anantha Ramakrishna, and J. B. Pendry, *Applied Physics Letters* **82**, 1506 (2003).
- <sup>22</sup>H. Shin and S. Fan, *Applied Physics Letter* **89**, 151102 (2006).
- <sup>23</sup>H. Shin and S. Fan, *Phys. Rev. Lett.* **96**, 073907 (2006).